CrystEngComm

Accepted Manuscript

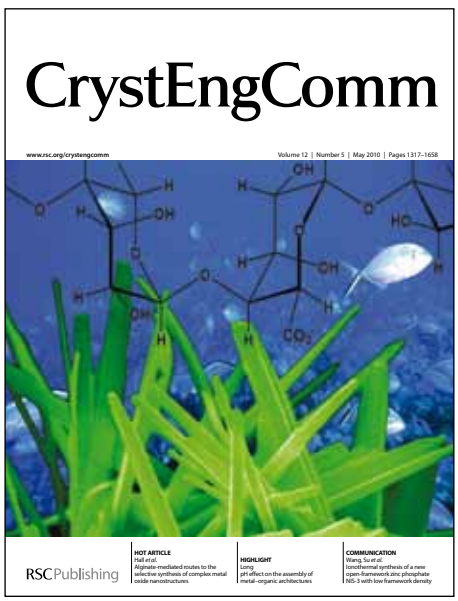

Journal Name

RSCPublishing

ARTICLE

Hydrogen-bond networks in polymorphs and solvates of metallorganic complexes containing ruthenium and aminoamide ligands

Cite this: DOI: 10.1039/x0xx00000x

A. Bacchi[a], G. Cantoni[a], D. Crocco[a], M. Granelli[b], P. Pagano[a], and P. Pelagatti[a] *

Received 00th January 2012,
Accepted 00th January 2012

DOI: 10.1039/x0xx00000x

www.rsc.org/

Half-sandwich ruthenium(II) complexes containing the two amino-amide ligands 4-aminobenzamide (4AB) and 4-aminobenzanilide (4ABN) have been synthesized and structurally characterized. The complexes have the general formula {[(p-cymene)RuCl2(κN-ligand)](x·solvent)}. The crystal packings are governed by extended hydrogen-bond networks involving the N-H bonds of the amine and amide groups as well as the Cl ligands. In the case of 4AB two different not solvate polymorphs (x = 0) have been isolated from methanol (**1α**) and water (**1β**, disappearing polymorph). In both cases the amide groups of two molecules associate giving rise to a supramolecular ring, where the N-H bond not involved in the ring contacts intermolecularly a neighbouring Cl ligand. The resultant frameworks result very robust thus impeding the insertion of solvent molecules. A methanol-solvate (**1·MeOH**) has in fact been isolated in very low yield where two methanols bridge two different amide groups. These crystals are highly unstable at room temperature. However, **1α** shows a distinct reactivity toward NH_3 in heterogeneous gas-uptake experiments, although the final nature of the product has not yet been defined. A comparison between the structural results here reported with those previously collected with 4-aminobenzoic acid reveals that the COOH function leads to linear supramolecular wheel-and-axle motifs, while the C(O)NH2 function of 4AB leads to bent supramolecular wheel-and-axle motifs. The complexes containing 4ABN (**2** and **2·2H₂O**) has always been crystallized as solvate (**2·EtOH** and **2·H₂O**), where the included guest molecules is hydrogen-bonded to the C(O)NHR functionality, thus preventing the dimerization of the amide groups.

Introduction

The intermolecular cyclic dimerization of COOH and $C(O)NH_2$ groups is one of the most common supramolecular synthons encountered in the solid state chemistry of carboxylic acids and primary amides.[1] These robust homomeric dimers have been used to fabricate highly ordered crystalline architectures with tunable properties.[2] Among the diverse molecular morphologies which can be used to make functional materials, wheel-and-axle compounds (waa), that is dumbbell shaped molecules formed by a central axle connecting two relatively bulky end units, are a promising class of compounds.[3] In fact, due to their irregular morphology they tend to frustrate the close-packing principle, thus giving rise to flexible crystalline networks with a high propensity to generate solvates or clathrates. We have recently shown that the cyclic dimerization of carboxylic functions of 4-aminobenzoic acids, such as 4-aminobenzoic acid (4ABA) and 4-aminocinnamic acid (4ACA), can be conveniently used to make the central axle of waa systems where the terminal wheels are represented by half-sandwich Ru(II) units $[(arene)RuCl_2]$,[4] as depicted in Scheme 1 for 4ABA.

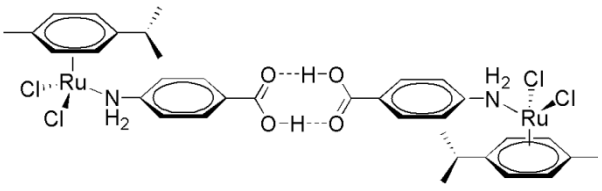

Scheme 1 Waa motif observed with half-sandwich Ru complexes with 4ABA.

For these organometallic compounds the amine function does not serve exclusively to bind the metal, but it exerts a basic role

in the construction of the desired crystal packing. In fact, the N-H bonds engage the hydrogen-bond acceptors chloride ligands[5] in intermolecular N-H…Cl-Ru hydrogen bonds, thus preventing their involvement in intermolecular Ru-Cl…H-OOC hydrogen bonds which would impede the creation of the desired supramolecular motif.[6] The clathrating properties of the isolated waa compounds are strongly dependent on the length

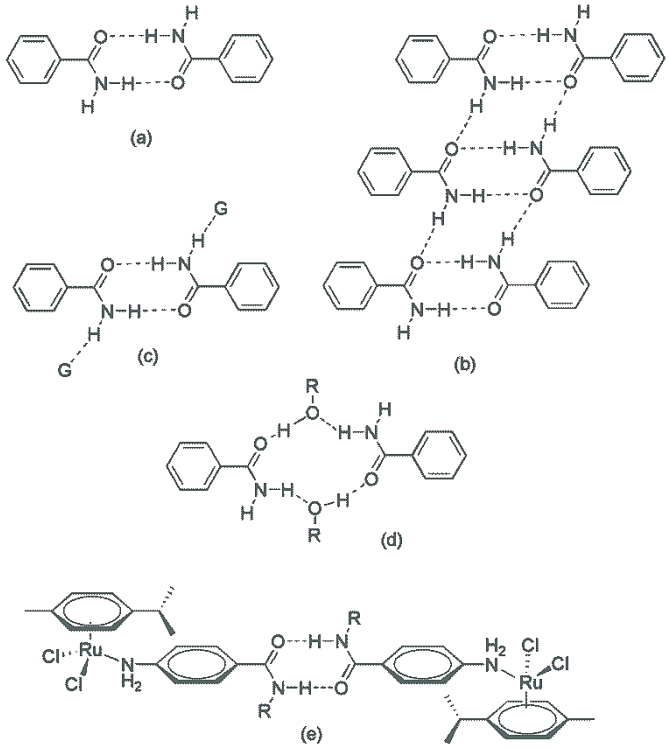

Scheme 2 Hydrogen bond networks for primary amides (benzamide in a-d) and representation of the organometallic waa complexes containing aminoamide ligands (e).

of the supramolecular spacer which in turn dictates the roominess of the cavities present in the lattice, as demonstrated by the possibility of obtaining solvates only with 4-aminocinnamic acid. The complex containing 4ABA is instead completely insensitive to a number of different hydrogen-bond donor/acceptor solvents, such as methanol, THF, acetone and water. Another successful strategy for the capture of organic guests by organometallic waa complexes is the functionalization of the aromatic ring of the aminobenzoic acid ligand with an OH functionality.[7] With 3-amino-4-hydroxybenzoic acid in fact, the corresponding Ru-based organometallic waa complex readily forms an acetone solvate where the guest is captured through an intermolecular O-H…O=CMe_2 hydrogen bond, both during crystallization of the not-solvate complex from acetone and absorption of vapours of acetone by the crystalline not-solvate complex (uptake). Taking this into account, it turned interesting to investigate the possibility of building organometallic waa compounds by using 4-aminobenzamide (4AB) as ligand (Scheme 2e, R = H) and then study their clathrating behaviour. For primary amides, the homomeric dimers (Schemes 2a) usually develop ladder motifs which originate from intermolecular hydrogen-bonds between the NH_2 anti hydrogen of an amide function and the oxygen atom of an adjacent amide group (Scheme 2b), giving rise to a $R_4^2(8)$ motif. This can be destroyed by the presence of hydrogen-bond acceptor guests (G in Scheme 2c) which reduce the degree of association by involving the NH_2 anti hydrogen bond in intermolecular N-H…G hydrogen bonds. In some cases, the ring is destroyed by inclusion in the dimer of hydrogen-bond acceptor solvents, typically alcohols or water, which produce larger supramolecular rings indicated as $R_4^4(12)$ (Scheme 2d). In order to get insights into the effect that an amide substituent may have onto the crystal packing of this class of organometallic compounds, the study has been extended to the secondary amide 4-aminobenzanilide (4ABN, Scheme 2e, R = Ph). As regards secondary amides, the $R_2^2(8)$ supramolecular synthon is very common in molecules where the amide nitrogen is part of a cycle, such as in diazepine derivatives,[8] whereas is rather rare for acyclic amides,[9] and this adds value to the use of secondary amides for the construction of organometallic waa architectures.

In this paper the solid-state characterization of the half-sandwich ruthenium(II) complexes of the aminoamide ligands 4AB and 4ABN are then reported (Scheme 3). The solid state structure of 4AB does not show the cyclic dimers but rather a catemer like structure,[10] while for 4ABN the X-ray structure has not been reported. However, 4-amino-N-tolylbenzamides form chains with extended intermolecular hydrogen bond networks involving the amine and amide groups.[11] Then, a particular emphasis will be given to the structural motifs which describe the solid state association of the organometallic waa compounds, in order to verify if the expected supramolecular architectures are realized.

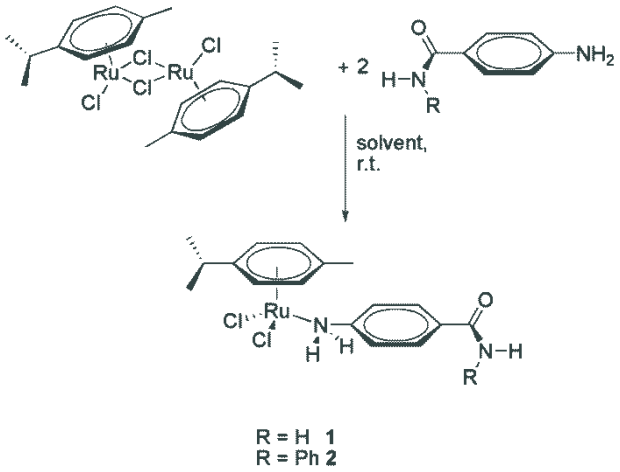

Scheme 3 Synthesis of the waa complexes

The possibility of generating solvate species by crystallization experiments or the possibility of inserting volatile guests in the crystal lattice by uptake will also be addressed. The abundance of amide functions in biological systems combined with the importance of the non-covalent interactions between discrete molecules for the understanding of biological chemistry processes, makes the study of amide containing complexes of particular relevance in the modern chemistry. This becomes even more true for half-sandwich Ru(II) complexes which are the subject of an intense bio-organometallic research.[12]

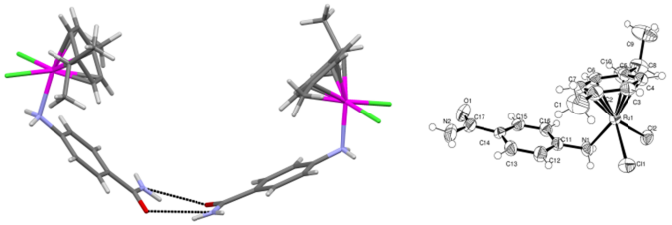

Figure 1 Right: molecular structure and labeling of [(p-cymene)Ru(κN-4AB)Cl_2]. Left: supramolecular dimerization of the amide functions found in the X-ray structure of **1α**.

Results and discussion

Ligand 4AB reacted with [(p-cymene)$RuCl_2]_2$ in methanol or water giving rise to the pseudo-octahedral complex [(p-cymene)Ru(κN-4AB)Cl_2] (**1α**) in good yield (Scheme 3). The FTIR-ATR spectra and XRPD traces of the two products isolated in the two solvents were identical, pointing out that the solvent has no effect on the nature of the final product. In **1α** ruthenium is in a pseudo-octahedral coordination environment, which is satisfied by the amine function of 4AB, by the two chloride ligands and by the η^6-coordinated p-cymene ring. The stoichiometry and purity of the isolated microcrystalline solids were confirmed by elemental analysis, which also indicated, together with TGA analysis, the absence of any trace of reaction solvent. Although FTIR spectroscopy has been used to elucidate the type of solid state intermolecular aggregation for primary amides,[13] a comparison of the FTIR spectra of complex **1α** and 4-aminobenzamide is not conclusive. In fact, the three bands at 3457, 3328 and 3320 cm^{-1} found for the free ligand are shifted to 3424, 3205 and 3148 cm^{-1} in the complex, with two additional small bands at 3346 and 3285 cm^{-1}. The bands at 3205 and 3148 cm^{-1} could indicate the formation of the intermolecular ring, but the signal at 3424 cm^{-1} is instead indicative of a catemer-like structure. The amide I band (C=O absorption) is centred at 1675 cm^{-1}, while two intense bands at 1609 and 1585 cm^{-1} are attributed to the deformation of the NH_2 groups. The C-N stretching band is visible at 1384 cm^{-1} as a strong band. These values, especially those belonging to the amide I stretching mode, are indicative of a strong degree of association of the amide group in the solid state.[14] The ^1H NMR spectrum recorded in CD_2Cl_2 containing one drop of deuterated dmso gave back the expected chemical shift signals (see Supporting Information for a detailed list of the NMR values). In order to decipher the type of synthon present in **1α**, crystals suitable for X-ray analysis were grown in methanol at -30°C. Complex **1α** bears three important supramolecular functionalities potentially active in the construction of the solid state arrangement: the amide NH_2, the amine NH_2, and the $RuCl_2$ groups. The structural analysis confirmed the pseudo-octahedral coordination for ruthenium and, importantly, the supramolecular dimerization of the amide functions with construction of the desired waa motif (Figure 1), which however appears unexpectedly bent.

In fact in **1α** the association of the amide functions by hydrogen bonds (N2…O1(i)= 2.952(7)Å, N-H...O=151(5)°, (i)= -x, y, -1/2-z) originates the $R_2^2(8)$ supramolecular synthon by application of a two-fold axis, while this motif is usually centrosymmetric, as in the case of the complexes of 4ABA,[4] where the two amine groups and the two COOH groups forming the central axle are co-planar. The reason for the bending must be ascribed to the rest of the packing architecture (see below). The other two significant supramolecular functions, the amine NH_2 and the $RuCl_2$ group, match together to build a strand of concatenated hydrogen bonded cages (Figure 2a) generated by a two-fold screw axis, and assisted also by CH…Cl short contacts (N1…Cl1(ii)=3.569(6)Å, 137(5)°; N1…Cl2(ii)=3.260(6)Å, 125(7)°; Cl1…C4(ii)= 3.717(6)Å; Cl2…C3(ii)=3.559(6)Å (ii)=1/2-x, 1/2+y,1/2-z). The XRPD diffractograms of the microcrystalline solids isolated form methanol and water are identical to the one calculated from the crystalline structure of **1α** (Figure S1 in the Supporting Information), thus pointing out that the waa system originates directly from synthesis in both protic solvents. While different association patterns between -NH_2 and -$RuCl_2$ have been already observed for the complexes of 4ABA[4] (Figure 2 inset), the present mode is unprecedented. As already observed in the series of complexes of 4ABA, we envisaged that the packing architecture should be based on the combination of the supramolecular motifs characteristic of the axle functionality ($R_2^2(8)$ amide in **1α**) (Scheme 2) convoluted with the association modes known for the NH_2 and the $RuCl_2$ groups, based on the patterns of NH…Cl interactions reported for the 4ABA family (Figure 2, inset), whose solid state behaviour was completely rationalized on the basis of these two orthogonal factors and of the perfect hydrogen bond balance. The present structure of **1α** reveals an important perturbation of the orthogonality, due to the mismatch of hydrogen bond donors and acceptors: the supramolecular axle (Figure 1) bears an unbalanced NH amidic group, unable to associate with the nearest C=O (as would be for Scheme 2b) since the adjacent molecules are kept apart as a consequence of the formation of the aminic NH…Cl-Ru cage (Figure 2).

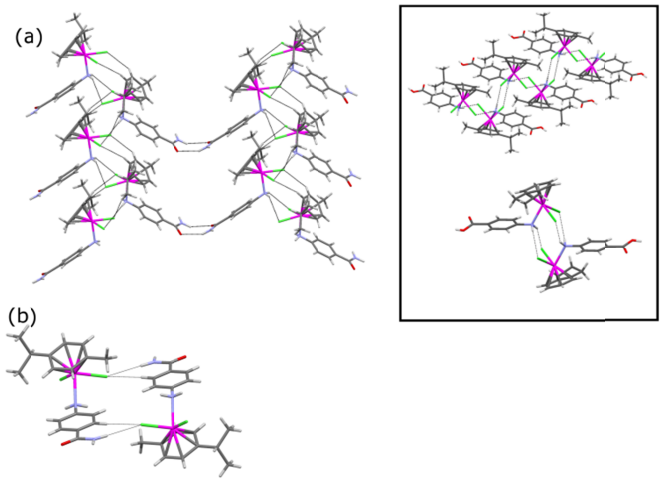

Figure 2 (a) Supramolecular packing motifs for 1α: the waa structure and the (amine)NH2…Cl interactions; (b) centrosymmetric interaction formed by the amidic NH group. Inset: (amine)NH2…Cl motifs observed in Ru-4ABA.[4]

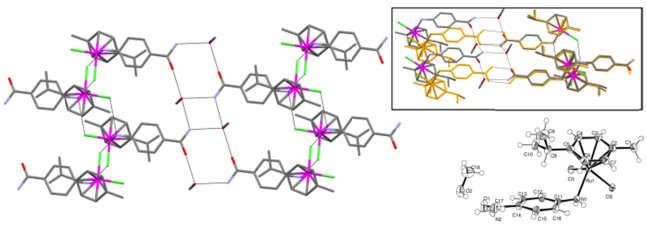

Figure 3 Left: supramolecular packing motifs for **1·MeOH**: the waa structure built by bridging MeOH and the (amine)NH2…Cl interactions. Right: molecular structure and labeling of **1·MeOH**. Inset: comparison between **1·MeOH** (element colour) and Ru-4ABA[4] (orange).

Hence the pending amidic NH group weakly interacts with a chlorine of the cage (N2…Cl1(iii)=3.589(8), 177(9)° (iii)=1/2-x, 3/2-y, -z, Figure 2b) and the aimed combination of motifs fails. This could also explain the IR pattern of **1α** which results, to some extent, intermediate between the catemer and dimer synthon. Most interestingly, the desired structure is obtained when a suitable guest is able to bridge between the pending amidic NH donor and the amidic C=O acceptor in **1·MeOH**, obtained as follows. After filtration of the crystals, the light orange solution was cooled at -30°C, isolating a few well shaped crystals suitable for X-ray analysis. In this case the crystals revealed to be unstable at room temperature, as demonstrated by their fast degradation once maintained exposed to the air for a few minutes. The X-ray data collection was then run at -100°C, revealing the incorporation of methanol into the crystal structure, with formation of complex **1·MeOH**. The observed decomposition of the crystals at room temperature is then imputable to methanol loss with consequent failure of crystallinity. In the X-ray structure of **1·MeOH** two methanol molecules bridge two amide functions belonging to two different organometallic units ($N2\ldots O2_{MeOH}$(iv) = 2.974(6)Å, 175(7)°; $O2_{MeOH}\ldots O1$= 2.705(6)Å, 168(7)°; $N2\ldots O2_{MeOH}$(v)=3.158(7)Å, 171(6)°; (iv)=2-x,-1-y,-z; (v)=x-1, y, z) giving rise to the $R_4^4(12)$ supramolecular synthon depicted in Scheme 2d (Figure 3). The aminic NH_2 and $RuCl_2$ units are engaged in the formation of a hydrogen bonded strand identical to the one observed for the similar complex of 4ABA based on NH…Cl hydrogen bonds (N1…Cl2(vi)=3.322(5)Å, 171(6)°; N1…Cl1(vii)=3.325(4)Å, 161(4)°; (vi)=-x, -y, 1-z; (vii)=1-x,-y,1-z), so that the overall structural arrangement is the same as in Ru-4ABA (Figure 3, inset), that presents also a similar unit cell and space group (a=7.745(3), b=9.175(4), c=14.900(7)Å, α 88.982(4) β=77.227(5) γ=70.695(4)°, P-1).

Unfortunately, the low number of crystals combined with their instability did not allow further characterization of the complex. Crystals suitable for X-ray analysis were also collected by slow evaporation of a saturated water solution of **1α**. The X-ray analysis revealed a polymorphic form of complex **1α**, here named **1β**, whose crystal structure determination presented some intricacy due to apparent pseudosymmetry and twinning, as described in the Experimental Section. **1β** is surprisingly related to **1α**: the complex are arranged exactly in the same layer built by the supramolecular bent waa dimerization of the amidic groups and by the strand of concatenated hydrogen bonded cages based on (amine)NH…Cl interactions and CH…Cl (Figure 4).

Subsequent recrystallizations from water always led to **1α** and then **1β** must be considered an example of disappearing polymorph.

The reaction between the ligand 4ABN and [(p-cymene)$RuCl_2$]$_2$ in dichloromethane in a ligand/dimer = 2:1 molar ratio at room temperature led to the fast precipitation of a microcrystalline orange solid whose elemental analysis was in agreement with the formula [(p-cymene)Ru(κN-4ABN)Cl_2]·$2H_2O$ (**2·2H$_2$O**, Scheme 3, R = Ph). The hydrate nature of the complex was further confirmed by TGA analysis. From the mother liquors refrigerated at -30 °C a second product precipitated, whose elemental analysis was in agreement with an anhydrous form (**2**), as further confirmed by TGA. The comparison of the XRPD diffractograms of the two complexes showed a much lower crystallinity for the anhydrous complex (see Supporting Information), whose diffractogram is almost featureless in the 2θ range 0-40°, except for an intense peak at 2θ = 11.3°. The FTIR-ATR spectra of complexes **2** and **2·2H$_2$O** are significantly different. In fact, in the high wavenumbers region the signals are identical except for two broad bands at 3540 cm^{-1} and 3342 cm^{-1} which are present only in the spectrum of **2·2H$_2$O** and which are then attributed to the OH stretching signals of the water molecules.

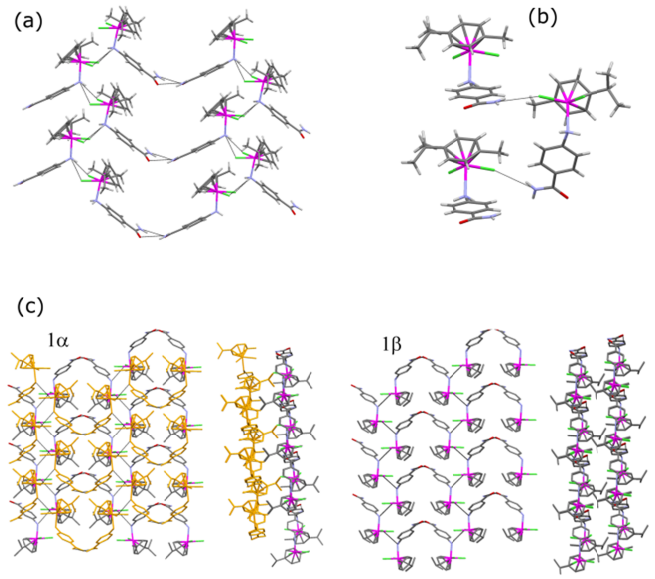

Figure 4 Structural arrangement found in **1β**: (a) the bent waa structure and the (amine)NH_2…Cl interactions; (b) interaction formed by the amidic NH group generated by a pseudo binary screw axis; (c) comparison of the layer arrangement in **1α** (left) and **1β** (right); two layers are displayed, in **1α** distinguished by colour.

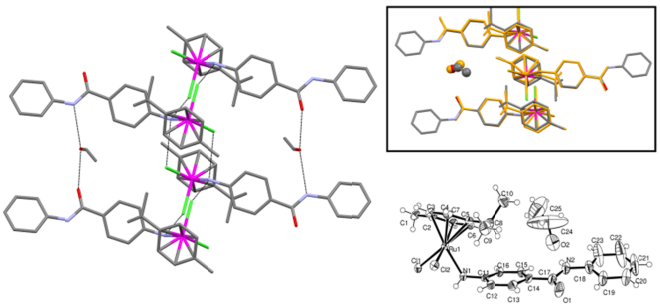

Figure 5 Left: supramolecular packing motif for **2·EtOH**: (amine)NH2…Cl interactions. Right: molecular structure and labeling of **2·EtOH**. Inset: structural similarity between **2·EtOH** (element colour) and **1·MeOH** (orange).

As regards the ν(C=O) of the amide group, the value found for complex **2** is practically coincident with that recorded for complex **1α** (1675 cm^{-1}), result which suggests the dimerization of the amide functions. For the hydrate complex **2·2H_2O** the ν(C=O) band is instead centred at a considerably lower value (1657 cm^{-1}). The observed lowering could be indicative of the involvement of the carbonyl group in intermolecular hydrogen-bonds with the included water molecules (see the Crystallographic Discussion for complex **2·H_2O**). In both cases a pseudo-octahedral coordination was assumed for ruthenium, with the η^6-coordinated arene ligand, the two chloride ligands and the amine function completing the coordination sphere. Both complexes were stable at room temperature for weeks, without signs of decomposition. Unfortunately, repeated attempts to crystallize complex **2** were unsuccessful, while crystals suitable for X-ray analysis were collected from recrystallization experiments of **2·2H_2O** conducted in water, methanol and ethanol (slow evaporation of saturated solutions). The crystals grown in water and methanol were a monohydrate complex (**2·H_2O**), while from ethanol **2·EtOH** was retrieved. The structure of the latter can be related to **1·MeOH** and to the Ru-4ABA and confirms the robustness and potential orthogonality of the structural motifs derived from the amide group on one hand, and from the aminic NH_2 and metal-bound chloride on the other: in **2·EtOH** the same aggregation pattern between NH_2 and $RuCl_2$ is observed (N1…Cl1(ix)= 3.290(1)Å, 167(1)°; N1…Cl2(x)=3.293(1)Å, 155(1)°; (ix)=2-x, 2-y, 2-z; (x) = 1-x, 2-y, 2-z), while EtOH bridges consecutive amidic functions (N2…$O2_{EtOH}$=3.116(1)Å, 172(1)°; $O2_{EtOH}$…O1(viii) = 2.765(1) Å, 173(1)°(viii)=x+1, y, z), as already found in **1·MeOH** (Figure 5). Apart from the supramolecular dimerization of the amide, impeded here by the aryl substituent, the structure of **2·EtOH** is equivalent to Ru-4ABA and to **1·MeOH** (Figure 5 inset), as the alcoholic guest does not alter the balance between hydrogen bond acceptors and donors, but acts as a linker that consolidates the pattern dictated by the NH…Cl-Ru interactions.

The structure of **2·H_2O** is profoundly affected by the alteration of the balance in the hydrogen bond network brought by water, that destroys both the arrangement of the NH…Cl-Ru motif and the amide concatenation. Two symmetry related water molecules are inserted in the NH…Cl-Ru cage (Figure 6) (N1…O2=3.101(3)Å, 175(2)°; O2…Cl1=3.386(3)Å, 139(2)°; N1…Cl1(xi)=3.441(2)Å, 137(2)°; O2…Cl2(xi)=3.169(2)Å, 143(3)°; (xi)=2-x, -1-y,1-z) while at the same time water accepts another hydrogen bond from the amidic N-H (N2…O2(xii)=3.110(3)Å, 162(2)°, (xii)=x, y+1, z). Water is in fact a better hydrogen bond partner than alcohols, and therefore it associates with the best hydrogen bond donors (NH) and acceptors (Ru-Cl) present in in the organometallic building-block, while the amidic C=O is not involved in the network.

Behaviour of complex 1α under NH_3 atmosphere

Despite the apparent lack of porosity, complex **1α** showed a distinct response to ammonia. When a microcrystalline sample of the complex was placed in a closed vessel saturated with the vapours of a concentrated solution of ammonia, the starting sample changed colour from orange to yellow within 25 minutes.

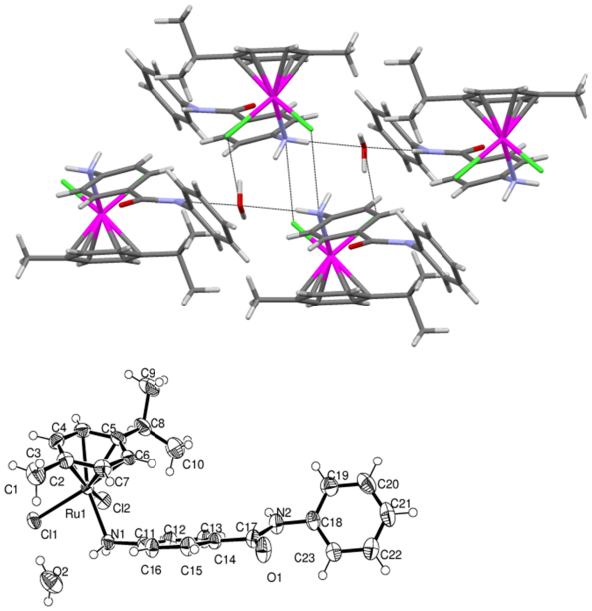

Figure 6 Top: supramolecular packing motif for **2·H$_2$O**: (amine)NH$_2$…H$_2$O…Cl interactions. Bottom: molecular structure and labeling of **2·H$_2$O**.

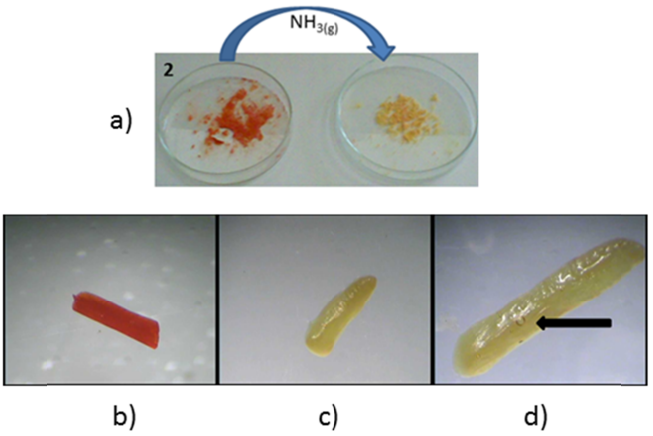

Figure 7 Top: colour change observed during the uptake of vapours of "anhydrous" ammonia by complex **1α**. Bottom: Single crystal of **1α** before (b) and after (c) ammonia uptake. d) Visualization of bubbles during the crystal liquefaction.

A prolonged exposure resulted in the partial liquefaction of the microcrystalline sample which became intractable. When the vapours of the aqueous ammonia solution were passed through a CaO trap before coming in contact with the complex, the solid became yellow without liquefaction (Figure 7a). However, once the sample was removed from the reactor and put in contact with air, the yellow microcrystalline solid liquefied within a few minutes with formation of an intractable mass. The sample remained intact when stored under nitrogen. This behaviour is indicative of a high hygroscopicity of the isolated compound, differently from the precursor **1α** which is completely inert towards water vapour uptake. Uptake experiments performed with volatile amines, such as triethylamine and diisopropylamine, led to formation of sticky light-brown solids which were not characterized. The ammonia uptake led to a microcrystalline product, as confirmed by an XRPD analysis conducted on a fresh sample under a nitrogen atmosphere (Figure S2 in the Supporting Information). Unfortunately, the high instability of the yellow compound prevented the recording of the elemental analysis. The FTIR-ATR spectrum of the yellow solid showed an enlargement of the N-H stretching band, compatible with the adsorption of ammonia (Figure S3 in the Supporting Information). Regrettably, repeated uptake experiments conducted on X-ray quality single crystals failed owing to crystal liquefaction during mounting on capillary, and then we are unable to pinpoint the NH_3 in the structure. A close inspection of the degraded yellow crystals showed the appearance of bubbles into the crystal bodies, which can be related to a fast ammonia release (Figure 7a-c).

Although half-sandwich Ru-complexes containing NH_3 are described as orange-yellow compounds, on the basis of the collected data we cannot identify the nature of the product which forms under ammonia atmosphere. However, the observed reactivity strongly indicates the structural dynamic and flexibility of the channel-free host network or **1α**.

Experimental Section

Although not strictly necessary, all the reactions were performed under dry nitrogen using standard Schlenk techniques. Glassware was oven-dried and cooled under a flux of nitrogen. Solvents were distilled prior to use and stored over molecular sieves, if not diversely stated. All the ligands are commercially available (Sigma-Aldrich) and were used as received. [(p-cymene)RuCl$_2$]$_2$ was prepared by a literature reported method.[15] The FTIR-ATR spectra were recorded by using a Nicolet-Nexus (ThermoFisher) spectrophotometer with a diamond ATR-crystal (4000-400 cm^{-1}). Elemental analyses were performed by using a FlashEA 1112 Series CHNS-O analyser (ThermoFisher) with gas-chromatographic separation. Powder XRD patterns were collected using Cu Kα radiation with a Thermo ARL X'TRA powder diffractometer equipped with a Thermo Electron solid state detector. TGA analyses were conducted by using a Perkin Elmer TGA7 apparatus.

Synthesis

[(p-cymene)RuCl$_2$(κN-4AB)] (1α) Method 1. [(p-cymene)RuCl$_2$]$_2$ (200 mg, 0.33 mmol) and 4-aminobenzamide (90 mg, 0.66 mmol) were placed in a Schlenk tube equipped with a magnetic bar. 40 ml of methanol were added and the resulting solution was stirred at room temperature for 24 hours and then refrigerated at -30 °C overnight. A yellow microcrystalline solid corresponding to **1α** was filtered off,

washed with diethyl ether and vacuum dried (222 mg, 75%). From the mother liquor refrigerated at -30 °C, crystals of **1α** suitable for X-ray analysis were collected. Mp (from MeOH): 238°C (dec.). Elemental Analysis. Found: C, 46.04; H, 4.99; N, 6.15. Calc. for $C_{17}H_{22}Cl_2N_2ORu$: C, 46.16; H, 5.01; N, 6.33. FTIR-ATR (ν_{max}/cm^{-1}): 3424, 3205, 3148, 1675, 1609, 1585, 1384. The mother liquors obtained after the second filtration were refrigerated at -30°C. Crystals suitable for X-ray analysis corresponding to **1·MeOH** were collected after one night of refrigeration. Method 2. The same amounts of reagents as in Method 1 were used, but water was used instead of methanol. $[(p\text{-cymene})RuCl_2]_2$ was added as solid to a water solution of the ligand, and the light red solution was stirred at room temperature for two hours. After refrigeration at 4 °C a light orange microcrystalline solid was filtered off, washed with diethyl ether and vacuum dried (256 mg, 54%). The spectroscopic characterization was identical to that of the product coming from methanol. For the sake of comparison the elemental analysis is reported. Elemental Analysis. Found: C, 46.11; H, 4.85; N, 6.21. Calc. for $C_{17}H_{22}Cl_2N_2ORu$: C, 46.16; H, 5.01; N, 6.33. The collected XRPD traces of the products isolated with the two methods were identical to that calculated from the X-ray structure of **1α**.

By slow evaporation of a saturated solution of **1** in water crystals suitable for X-ray analysis were collected corresponding to **1β**. Subsequent recrystallizations of **1** in water always led to **1α**.

[(p-cymene)RuCl$_2$(κN-4ABN)] (2·2H$_2$O) Method 1. 4ABN (139 mg, 0.653mmol) was placed in a Schlenk tube equipped with a magnetic bar and dissolved in 10 ml of dichloromethane. $[(p\text{-cymene})RuCl_2]_2$ (200 mg, 0.327 mmol) was dissolved in 10 ml of dichloromethane, and the resulting red solution was transferred to the reactor containing the ligand solution. The resulting orange solution was stirred at room temperature for 24 hours, obtaining a microcrystalline orange solid, which was filtered off, washed with dichloromethane and vacuum dried for several hours (232 mg, 64%). Mp: 230 °C. Elemental Analysis. Found: C, 49.74; H, 5.18; N, 4.84. Calc. for $C_{23}H_{30}Cl_2N_2O_3Ru$: C, 49.82; H, 5.45; N, 5.05. FTIR-ATR (ν_{max}/cm^{-1}): 3540, 3342, 3291, 3204, 3110, 1657, 1596, 1535, 1508, 1439, 1318, 1261, 1239, 1104, 1085, 754, 695. TGA (nitrogen atmosphere, 25°C-200°C, 10°C/min^{-1}): expected loss = 6.50%; observed loss = 6.35%.

Well shaped single crystals suitable for X-ray analysis were grown by slow evaporation of saturated water (**2·H$_2$O**) and ethanol (**2·EtOH**) solutions.

From the mother liquors refrigerated at -30 °C, a second orange solid corresponding to **2** was filtered off, washed with diethyl ether and vacuum dried (50 mg, 15%). Elemental Analysis. Found: C, 53.29; H, 5.25; N, 5.14. Calc. for $C_{23}H_{26}Cl_2N_2ORu$: C, 53.27; H, 5.05; N, 5.40. FTIR-ATR (ν_{max}/cm^{-1}): 3302, 3212, 3115; 1672, 1642, 1598, 1543, 1509, 1441, 1320, 1262, 1238, 1103, 762, 694. The ^{1}H NMR spectrum recorded in CD_2Cl_2 was identical to that of complex **2·2H$_2$O**.

Method 2 4ABN (100 mg, 0.471 mmol) and $[(p\text{-cymene})RuCl_2]_2$ (145 mg, 0.236 mmol) were placed in a Schlenk tube equipped with a magnetic bar and dissolved in 40 ml of dry methanol. The solution was stirred at room temperature for 24 hours. The microcrystalline orange solid was filtered off, washed with methanol, diethyl ether and finally vacuum dried for several hours (159 mg, 61%). The characterization data were equivalent to those collected for complex **2·2H$_2$O**. By slow evaporation of a saturated methanol solution crystals suitable for X-ray analysis were collected (**2·H$_2$O**).

Ammonia uptake

30 mg of complex were placed in an open vial which was introduced in a tube of an H-cell (Figure S4 in the Supporting Information). In the second tube were introduced 10 ml of concentrated aqueous ammonia solution. The horizontal connector of the H-cell is furnished with two sintered glass filters which allow the introduction of a desiccant (CaO) in order to block the vapours of water during the uptake. After closure of the cell the apparatus was maintained at room temperature for the desired time.

Single Crystal X-ray Diffraction Analyses

Single crystal X-ray diffraction data were collected using the MoKα radiation (λ= 0.71073Å) for all compounds on a SMART APEX2 diffractometer at T = 293 K, except for **2·MeOH** and **2·EtOH** that were measured at 170 K to prevent decay. Lorentz, polarization, and absorption corrections were applied.[16] Structures were solved by direct methods using SIR97[17] and refined by full-matrix least-squares on all F^2 using SHELXL97[18] implemented in the WinGX package.[19] Hydrogen atoms were partly located on Fourier difference maps and refined isotropically and partly introduced in calculated positions. Anisotropic displacement parameters were refined for all non-hydrogen atoms, except for compound **1β**, where isotropic parameters for all atoms except for Ru and Cl and geometric constraints were used to model the structure. The structural determination of **1β** has been carried out in the P1 space group, with two independent molecules in the cell, related almost perfectly by a pseudo binary screw axis. The triclinic cell could be transformed to a cantered monoclinic one, where the two fold axis could have been a proper symmetry element, with dimensions related to half the cell of **1α** (**1β** transformed to I-cantered: a = 9.227, b = 8.723, c = 22.817 Å, α=89.876, β=96.087, γ=90.260°), but no consistent space group was identified for the cantered monoclinic setting. The final best model presents some problematic close contact involving terminal methyl groups, due to poor data quality. Hydrogen bonds have been analysed with SHELXL97[18] and PARST97,[20] and extensive use was made of the Cambridge Crystallographic Data Centre packages[21] for the analysis of crystal packing. Table 1 summarizes crystal data and structure determination results. Crystallographic data (excluding structure factors) for **1α**, **1β**, **1·MeOH**, **2·EtOH**, **2·H$_2$O** have been deposited with the Cambridge Crystallographic Data Centre as supplementary publication no. CCDC 941876-941880. Copies of the data can

be obtained free of charge on application to CCDC, 12 Union Road, Cambridge CB2 1EZ, UK (fax: (+44) 1223-336-033; e-mail: deposit@ccdc.cam.ac.uk).

Conclusions

The use of a primary amide group for the fabrication of supramolecular metallorganic waa compounds led to several structural motifs where the amide group plays different roles. The most robust supramolecular synthon revealed to be the cyclic supramolecular dimer, which formed even in protic solvents such as methanol and water. It is noteworthy that the binding of the $[(p\text{-cymene})RuCl_2]_2$ moiety leads to the supramolecular dimerization of the amide function, synthon not present in the X-ray structure of the free ligand 4AB which instead crystallizes in a catemer like structure.[13] Contrarily to what often observed with primary amides the N-H bond not involved in the supramolecular dimerization is not prone to interact with hydrogen-bond donor/acceptor guests, such as methanol and water, since it is actively involved in an intermolecular contact with a chloride ligand of a neighbouring molecule. Only in a minor product the involvement of MeOH was observed (**1·MeOH**) although the solvent is not captured by the N-H amide bond but it is inserted in the supramolecular dimer enlarging the corresponding ring to an $R_4^4(12)$ motif. The use of a secondary amide group did not bring to the formation of a supramolecular dimer, rather to solvates where the guest molecule is captured by the C=O (ethanol, **2·EtOH**) or the N-H (water, **2·H_2O**) amide bonds. Then, for this class of organometallic compounds the use of secondary amide groups results more successful for the capture of hydrogen bond donor/acceptor guests than the use of primary amide functions. However, the unique behaviour shown by **1α** toward ammonia underlines the dynamic behaviour of this channel free organometallic waa compound. The nature of the final product which forms from the ammonia uptake and the mechanism through which the gaseous guest enters into the crystalline framework are currently under investigation in our laboratory.

Acknowledgements

The *Laboratorio di Strutturistica "M. Nardelli"* and the *CIM* (*Centro Interdipartimentale di Misure*) of the University of Parma are thanked for technical assistance and instrument facilities. Dr. Ferdinando Vescovi of the Department of Chemistry of the University of Parma is thanked for XRPD analyses.

Notes and references

[a] Dipartimento di Chimica, Università degli Studi di Parma, Parco Area Scienze 17/A, 43124 Parma, Italy. Tel. +390521905426. Fax +390521905557. E-mail paolo.pelagatti@unipr.it

[b] Department of Chemistry, University of Genève, Quai Ernest A. 30, 1205, Genève, Switzerland.

Electronic Supplementary Information (ESI) available: [XRPD traces of **1** and of the ammonia uptake product; comparison of the FTIR spectra of **1α** and the ammonia uptake product; figure of the H-reactor used for the ammonia uptake; crystallographic data in the CIF format of compounds **1α**, **1β**, **1·MeOH**, **2·EtOH** and **2·H_2O**.]. See DOI: 10.1039/b000000x/

Table 1 Crystal data and structure refinement for **1α, 1β, 1·MeOH, 2·EtOH, 2·H_2O**

	1α	**1β**	**1·MeOH**	**2·EtOH**	**2H_2O**
Empirical formula	$C_{17}H_{22}Cl_2N_2ORu$	$C_{17}H_{22}Cl_2N_2ORu$	$C_{18}H_{26}Cl_2N_2O_2Ru$	$C_{25}H_{32}Cl_2N_2O_2Ru$	$C_{23}H_{30}Cl_2N_2O_2Ru$
Formula weight	442.34	442.34	474.38	564.50	536.44
Temperature (K)	293(2)	293(2)	170(2)	170(1)	293(2)
Wavelength (Å)	0.71073	0.71073	0.71073	0.71073	0.71073
Crystal system	monoclinic	triclinic	triclinic	triclinic	triclinic
Space group	C2/c	P1	P-1	P-1	P-1
	a = 25.574(2)	a = 8.723(9)	a = 7.766(1)	a = 7.6649(9)	a = 9.516(5)
	b = 8.7383(8)	b =9.227(9)	b = 9.144(1)	b = 9.071(1)	b = 9.814(5)
	c = 18.346(2)	c =12.62(1)	c = 15.613(2)	c = 19.817(2)	c = 14.001(5)
		α= 74.26(1)	α= 83.304(3)	α= 87.882(2)	α= 74.216(5)
	β= 116.964(1)	β= 69.80(1)	β= 82.977(3)	β= 89.682(2)	β= 82.094(5)
		γ = 89.74(1)	γ = 69.036(3)	γ = 70.084(2)	γ = 67.846(5)
Volume ($Å^3$)	3654.2(6)	913.0(15)	1024.4(2)	1294.5(3)	1164.5(9)
Z	8	2	2	2	2
Density (calculated) (Mg/m^3)	1.608	1.609	1.538	1.448	1.530
Absorption coefficient (mm^{-1})	1.155	1.156	1.039	0.835	0.924
F(000)	1792	448	484	580	548
θ range (°)	1.79 - 26.41	1.80 - 18.93	1.32 - 26.45	1.03 - 23.29	1.51 - 31.83
Reflections collected	17802	4107	11534	8648	19231
Independent refl. [R(Int)]	3740 [0.0437]	2816 [0.0754]	4192 [0.0611]	3734 [0.0313]	7426 [0.0267]
Refinement method	Full-matrix LS on F^2	Full-matrix LS on F^2	Full-matrix LS on F^2	Full-matrix LS on F^2	Full-matrix LS on F^2
Data / restraints / parameters	3740 / 2 / 227	2816 / 74 / 167	4192 / 0 / 319	3734 / 0 / 305	7426 / 3 / 290
Goodness-of-fit on F^2	1.205	1.500	1.005	0.902	1.068
Final R, wR2 [I>2σ (I)]	0.0448, 0.0929	0.1265, 0.3327	0.0477, 0.1224	0.0274, 0.0658	0.0267, 0.0671
R, wR2 (all data)	0.0806, 0.1171	0.1761, 0.3864	0.0553, 0.1261	0.0347, 0.0692	0.0295, 0.0684
Largest ΔF max/min ($e.Å^{-3}$)	1.458 / -0.870	2.171 / -1.314	2.550 / -1.399	0.448 / -0.395	0.415 / -0.786

1 T. Beyer, S. L. Price, *J. Phys. Chem. B*, 2000, **104**, 2647.
2 R. K. R. Jetti, S. S. Kuduva, D. S. Reddy, F. Xue, T. C. W. Mak, A. Nangia, G. R. Desiraju, *Tetrahedron Lett.*, 1998, **39**, 913; Z. Quin, M. C. Jennings, R. J. Puddephatt, K. W. Muir, *Inorg. Chem.*, 2002, **41**, 5174; S. E. Dann, S. E. Durran, M. R. J. Elsegood, M. B. Smith, P. M. Staniland, S. Talib, S. H. Dale, *J. Organomet. Chem.*, 2006, **691**, 4829.
3 D. V. J. Soldatov, *J. Chem. Cryst.*, 2006, **36**, 747.
4 A. Bacchi, G. Cantoni, M. Granelli, S. Mazza, G. Rispoli, *Cryst. Growth Des.*, 2011, **11**, 5039.
5 L. Brammer, E. A. Bruton, P. Sherwood, *Cryst. Growth Des.*, 2001, **1**, 277; L. Brammer, *Chem. Soc. Rev.*, 2004, **33**, 476; G. M. Espallargas, F. Zordan, L. A. Marín, H. Adams, K. Shankland, J. van de Streek, L. Brammer, *Chem.-Eur. J.*, 2009, **15**, 7554; C. J. Adams, F. Haddow, M. Lusi, A. G. Orpen, *Proc. Natl. Acad. Sci. U.S.A.*, 2010, **107**, 16033.
6 A. Bacchi, G. Cantoni, M. R. Chierotti, A. Girlando, R. Gobetto, G. Lapadula, P. Pelagatti, A. Sironi, M. Zecchini, *CrystEngCom*, 2011, **13**, 4365.
7 A. Bacchi, M. Carcelli, P. Pelagatti, *Crystallogr. Rev.*, 2012, **18**, 253; A, Bacchi, G. Cantoni, F. Mezzadri, P. Pelagatti, *Cryst. Growth Des.*, 2012, **12**, 4240.
8 S. W. Gordon-Wylie, E. Teplin, J. C. Morris, M. I. Trombley, S. M. McCarthy, W. M. Cleaver, G. R. Clark, *Cryst. Growth Des.*, 2004, **4**, 789; L. A. Chetkina, O. V. Semidetko, V. A. Shuvaeva, A. N. Poplavskii, V. K. Bel'skii, A. M. Andrievskii, *Zh. Struct. Khim. (J. Struct. Chem.)*, 1987, **28**, 177; Q.-B. Li, W.-C. Yang, Y.-J. Han, X.-J. Zhao, *Acta Crystallogr., Sect E: Struct. Rep. Online*, 2006, **62**, o3021; T. Olszewska, M. Gdaniec, T. Polonski, *J. Org. Chem.*, 2004, **69**, 1248; L. Baldini, F. Sansone G. Faimani, C. Massera, A. Casnati, R. Ungaro, *Eur. J. Org. Chem.*, 2008, 869; A. V. Samet, K. A. Kislyi, V. N. Marshalkin, Y. A. Strelenko, Y. V. Nelyubina, K. A. Lyssenko, V. V. Semenova, *Russ. Chem. Bull.*, 2007, **56**, 2089; O. V. Semidetko, L. A. Chetkina, V. K. Bel'skii, A. M. Andrievskii, A. N. Poplavskii, K. M. Duymaev, *Kristallografiya,* 1989, **34**, 106.
9 P. M. Diamond, S. E. Dinizio, R. W. Freerksen, R. C. Haltiwanger, D. S. Watt, *Chem. Commun.*, 1977, 298; R. Dalpozzo, A. De Nino, L. Maiuolo, A. Procopio, G. De Munno, G. Sindona, *Tetrahedron*, 2001, **57**, 4035; F. H. Beijer, R. P. Sijbesma, J. A. J. M. Vekemans, E. W. Meijer, H. Kooijman, A. L. Spek, *J. Org. Chem.*, 1996, **61**, 6371; R. J. Griffin, P. R. Lowe, *J. Chem. Soc., Perkin Trans. 1*, 1992, 1811; M. Ikaunieks, S. Belyakov, M. Madre, *J. Heterocycl. Chem.*, 2006, **43**, 943; J. A. Galvez, J. Quiroga, J. Cobo, C. Glidewell, *Acta Crsytallogr., Sect. C: Cryst Struct. Commun.*, 2010, **66**, o521.
10 Z. Berkovitch-Yellin, J. van Mil, L. Addadi, M. Idelson, M. Lahav, L. Leiserowitz, *J. Am. Chem. Soc.*, 1985, **107**, 3111.
11 N. E. C. Duke, P. W. Codding, *J. Med. Chem.*, 1992, **35**, 1806.
12 E. H. Hillard, G. Jaouen, *Organometallics*, 2011, **30**, 20; H.-K. Liu, P. Sadler, *Acc. Chem. Res.*, 2011, **44**, 349; W. H. Ang, A. Casini, G. Sava, P. J. Dyson, *J. Organomet. Chem.*, 2011, **696**, 989; M. Carcelli, A. Bacchi, P. Pelagatti, G. Rispoli, D. Rogolino, T. W. Sanchez, M. Sechi, N. J. Neamati, *J. Inorg. Biochem.*, 2013, **118**, 74.
13 A. Mukherjee, S. Tothadi, S. Chakraborty, S. Ganguly, G. R. Desiraju, *CrystEngCom*, 2013, **15**, 4640.
14 L.J. Bellamy, *The Infra-red Spectra of Complex Molecules*, Chapman and Hall, London, 1975; N. Blagden, R. Davey, G. Dent, M. Song, W. I. F. David, C. R. Pulham, K. Shankland, *Cryst. Growth Des.*, 2005, **5**, 2218; P. Pandey, A. K. Samanta, B. Bandyopadhyay, T. Chakraborty, *J. Mol. Struct.*, 2010, **975**, 343; H. Torii, T. Tatsumi, T. Kanazawa, M. Tasumi, *J. Phys. Chem.*, 1998, **102**, 309.
15 Bennet, M. A.; Huang, T. N.; Matheson, T. W.; Smith, A. K. *Inorg. Synth.* **1982**, 74-78.
16 SAINT: SAX, Area Detector Integration, Siemens Analytical instruments INC., Madison, Wisconsin, USA; SADABS: Siemens Area Detector Absorption Correction Software, G. Sheldrick, 1996, University of Goettingen, Germany.
17 Sir97: A new Program for Solving and Refining Crystal Structures – A. Altomare, M. C. Burla, M. Cavalli, G. Cascarano, C. Giacovazzo, A. Gagliardi, A. G. Moliterni, G. Polidori, R. Spagna, 1997, Istituto di Ricerca per lo Sviluppo di Metodologie Cristallografiche CNR, Bari.
18 Shelxl97. Program for structure refinement. G. Sheldrick, University of Goettingen, Germany, 1997.
19 L. J. Farrugia, *J. Appl. Cryst.*, 1999, **32**, 837.
20 M. Nardelli, *J. Appl. Cryst.*, 1995, **28**, 659.
21 F. H. Allen, O. Kennard, R. Taylor, *Acc. Chem. Res.*, 1983, **16**, 146; I. J. Bruno, J. C. Cole, P. R. Edgington, M. Kessler, C. F. Macrae, P. McCabe, J. Pearson, R. Taylor, *Acta Crystallogr.*, 2002, **B58**, 389.

Table of contents entry

Hydrogen-bond networks in polymorphs and solvates in metallorganic complexes containing ruthenium and aminoamide ligands

Alessia Bacchi, Giulia Cantoni, Domenico Crocco, Matteo Granelli,† Paolo Pagano, Paolo Pelagatti*

Dipartimento di Chimica, Università degli Studi di Parma, Viale delle Scienze 17/A, 43124 Parma, Italy

† Department of Chemistry, University of Genève, Quai Ernest A. 30, 1205 Genève, Switzerland

*Paolo Pelagatti, Department of Chemistry, University of Parma, Parco Area Scienze 17/A, 43124 Parma, Italy. Email paolo.pelagatti@unipr.it. Tel. +39 0521 905426. Fax +39 0521 905557

The hydrogen-bond networks of half-sandwich Ru(II) complexes containing primary and secondary amide groups are described together with their guest inclusion properties